RSC Advances

ROYAL SOCIETY OF CHEMISTRY

www.rsc.org/advances

Influence of Hexagonal Boron Nitride on Selective Catalytic Reduction of NO with NH_3 over CuO_X/TiO_2

Dongsheng Zhou[1], Zhiyuan Ren[2], Bo Li[1], Zhaoxia Ma[1], Xiaobin Zhang[1], Hangsheng Yang[1*]

[1]State Key Laboratory of Silicon Materials, Department of Materials Science and Engineering, Zhejiang University, Zheda Road 38, Hangzhou 310027, China

[2]Foreign Economic Cooperation Office, Ministry of Environmental Protection, China, No 5 HouyingfangHutong, Xicheng District, Beijing 100035, China

Abstract

Hexagonal boron nitride (hBN) was used as CuO_X/TiO_2 catalyst carrier and its effect on NO reduction with NH_3 was studied. After hBN was treated with concentrated HNO_3, CuO_X/TiO_2 nanoparticles were dispersed well on hBN, and the addition of hBN was found to promote NO oxidation, at the same time suppress the NH_3 oxidation to NO, thus promoted the selective catalytic reduction of NO at reaction temperature between 150 to 350 °C, and high De-NO_X efficiency of 90.6% was achieved at 275 °C. Our study indicates that hBN is a promising catalyst promoter and carrier with excellent stability compared to carbonaceous materials.

Keywords: SCR; copper oxide; TiO_2; hBN

*To whom correspondence should be addressed. Tel/Fax: +86-571-87951404;

E-mail: hsyang@zju.edu.cn

1 Introduction

The control of nitric oxides (NO_X) emission from fuel combustion processes, which cause harmful effects on ecosystem and humanity, has received increasingly concern. Selective catalytic reduction (SCR) has been proved to be one of the most effective methods for NO_X emission reduction [1] A variety of catalysts have been investigated, including noble metals [2-4], ion-exchanged zeolites [5-7], and metal oxides [8, 9]. Especially, V_2O_5-WO_3/TiO_2 based catalysts have been commercial applied despite their toxicity [10, 11]. It is therefore necessary to develop novel catalysts to replace vanadium. Among them, Cu-zeolite based catalysts with low toxicity have been extensively investigated as SCR catalysts using NH_3- and HC-SCR of NO_X, which showing promising properties due to their high thermal stability and hydrocarbon resistance [12, 13]; though they deactivated rapidly by moisture and SO_2 at low temperatures [14].

Besides the catalyst optimization, catalyst carriers and/or promoters are also important for good SCR performance. For example, copper oxides support on Al_2O_3 [15], TiO_2 [16], SiO_2 [17], ZrO_2 [18], carbonaceous materials [19] or their composites [20-22] have been extensively investigated as SCR catalysts, especially carbonaceous materials have been systematically studied recently as carrier/promoter for their large surface area and good adsorption of NO_X [23, 24]. Nevertheless, due to their instability under high temperature and oxygen enriched conditions, the carbon-based catalysts could be difficult to adapt to the complex exhaust gases at relative high temperature. Hexagonal boron nitride (hBN), being isostructural with graphite, presents a higher

stability towards oxidation than carbon, which makes it a promising candidate for catalyst support under extreme operating conditions [25], even as-deposited ultrathin hBN films are stable in the presence of metallic catalysts in oxygen-rich environments below 500 °C [26, 27]. In addition, hBN is hydrophobic, preventing moisture condensation on its surface [28]. But few results using hBN as carrier/promoter have been reported, in fact it was reported that the dispersion of active components, especially metal oxides, on hBN is poor, which hindered to its application [29]. In this study, we found that using a sol-gel method, CuO_X/TiO_2 nanoparticles could be well dispersed on nitric acid pretreated hBN. As a result, high performance of selective catalytic reduction of NO was achieved over the good dispersed CuO_X/TiO_2-hBN catalysts.

2 Experimental

2.1 Catalyst preparation

Hexagonal BN (99.9% metals-basis, Aladdin) were pretreated in concentrated HNO_3 at 60 °C for 3h, the suspensions were filtrated, washed with distilled water until the pH reached up to 7, and the obtained precipitates were dried at 100 °C for later use. The catalysts were prepared by classical sol-gel method. Pretreated hBN were first stirred in ethanol for good dispersion, and tetrabutyl titanate was added (keeping stirring). Then copper nitrate and acetic acid, in distilled water and ethanol, was added into the above solution, and the resulted solution was stirred until sols were formed. The sols were aged at ambient conditions to obtain good gels, and then dried at 100 °C overnight and calcined at 500 °C for 4 h in a N_2 atmosphere to acquire CuO_X/TiO_2-

hBN. Four samples with different hBN concentrations and same Cu loading were prepared to investigate the effect of hBN on SCR of NO by NH_3, as shown in Table 1.

2.2 Catalyst characterization

X-ray diffraction (XRD) patterns were recorded on a Philips XD-98 X-ray diffractometer with Kα radiation (λ= 0.15406 nm). A Hitachi S-4800 scanning electron microscope (SEM) was used to characterize the morphology of the samples. Brunauer–Emmett–Teller (BET) surface areas were measured using an ASAP2000 physical adsorbent. X-ray photoelectron spectroscopy (XPS) data were obtained using a Thermo ESCALAB 250, the X-ray source was an Al Kα radiation, and all binding energies were referenced to the 284.8 eV C1s.

H_2-temperature-programmed reduction (H_2-TPR) experiments were performed using 100 mg of each catalyst. The samples were pretreated in helium from 40 °C to 400 °C at a temperature increment of 10 °C/min. TPR experiments were performed at a heating rate of 10 °C/min under a mixed flow of 10% H_2 in helium at a flow rate of 30 ml/min. NH_3-temperature-programmed desorption (NH_3-TPD) experiments were performed using 200 mg of each catalyst to determine their NH_3 adsorption ability. The sample was pretreated in a N_2 stream (30 ml/min) at 400 °C for 1 h, and then cooled to 100 °C. The pretreated sample was exposed to a mixed flow of 4% NH_3 in Ar at a flow rate of 20 ml/min for 3 h at ambient temperature, and then heated from 100 °C to 850 °C at a heating rate of 10 °C/min. The H_2-TPR and NH_3-TPD data were recorded using an on-line gas chromatograph equipped with a thermal conductivity detector.

NO-temperature-programmed oxidation (NO-TPO) experiments were performed in a fixed-bed flow reactor using an NO-NO_2-NO_X analyzer (Testo AG testo 350) to record the NO and NO_2 signals. The catalysts were pasted on three Al plates and inserted into the fixed-bed [19], then it was heated from 80 °C to 420 °C, and 800 ppm of NO was fed in the presence of oxygen (5.4 %, v/v) and a N_2 balance at a total flow rate of 1000 sccm and a gas hourly space velocity (GHSV) of 75,000 h^{-1}.

NO-temperature-programmed desorption (NO-TPD) and NO_2-temperature-programmed desorption (NO_2-TPD) experiments were performed on the catalysts using Testo AG testo 350 to record the NO and NO_2 signals. The samples were exposed to a 800 ppm NO flow and 5.4 vol% O_2 for 2 h at 400 °C and cooled to 100 °C in the same gas stream, followed by a N_2 purge during sample cooling to 80 °C. Once the NO signal returned to the baseline level, the temperature was ramped from 80 °C to 420 °C in N_2 at a rate of 10 °C /min.

2.3 Catalyst activity test

The catalytic activity tests were carried out in the same fixed-bed flow reactor with 1.2 g catalyst samples pasted on three Al plates (4 cm × 10 cm) [30]. The simulated gas for these tests contained 800 ppm NO, 800 ppm NH_3 and 5.4 vol% O_2 balanced by N_2 at total flow rate of 1000 sccm from 100 °C to 400 °C and a GHSV of 75,000 h^{-1}. The inlet and outlet concentrations of NO and NO_2 were monitored using Testo AG testo 350.

3 Results and discussion

3.1 Catalyst activity

Catalytic activities of NO removal over CuO_X/TiO_2-hBN catalysts are shown in Fig. 1(a). The catalytic performance over all catalysts displayed same volcano shaped plots, which could be divided into four stages: the NO conversions all increased with temperature gradually up to 150 °C; and then rapidly increased and reached up to the maximum values at 275 °C; the quick decrease of activity at temperature from 300 °C to 375 °C could be due to the side reaction of NH_3 oxidation [31]; at temperature above 375 °C, the catalytic activities almost lost completely. The Cu-Ti presented the lowest activity for the reduction of NO_X in the investigated window (100-400 °C), which was in agreement with the previous reports [31, 32]. The addition of hBN promoted the NO conversion evidently, the maximum of 90.6% NO conversion was achieved over Cu-Ti-BN-10, compared with 73.2% over Cu-Ti. However, when hBN was further increased to 15 wt%, the catalytic activity decreased again, this could be due to the decrease metal oxides dispersion caused by hBN agglomeration, which was supported by BET surface area decrease from 78.1 to 73.5 m^2/g as shown in Table 1.

To simplify the complicated surface reaction, kinetic parameters were calculated from NO conversion based on the following equations (1-2) on assumption that the reaction is first-order dependent on NO and zero-order dependent on NH_3 [33, 34].

$$k = -\frac{V}{M} \cdot \ln(1-x) \quad (1)$$

$$k = A \cdot \exp\left(\frac{Ea}{RT}\right) \quad (2)$$

Where k is the reaction rate coefficient (mL/g/s), V is the total gas flow rate (mL/s), M is the mass of the catalyst (g), x is the conversion of NO_X (%), Ea is the apparent activation energy (J/mol), A is the pre-exponential factor, R is the gas constant (8.3145

J/mol/K), and T is the reaction temperature (K).

As shown in Fig. 1(b), the reaction constant over Cu-Ti-BN-10 was as high as 33 mL/g/s, compared with other catalysts. The apparent activation energies (Ea) were calculated according to equation (2) and shown in the inset of Fig. 1(b) and Table 2. The increase of k and decrease of Ea indicated a remarkable promotion for NO catalytic reduction with the introduction of hBN.

3.2 XRD analysis and SEM observation

Fig. 2 shows the XRD patterns of hBN and CuO_X/TiO_2-hBN catalysts. From the XRD peaks, it is evident that TiO_2 existed as anatase phase (25.3°). Besides, a hexagonal structure (26.8°) was kept in hBN. The peaks at 35.5° and 38.7° corresponding to CuO_X appeared in all CuO_X/TiO_2-hBN catalysts. Typical SEM images of the Cu-Ti and Cu-Ti-BN-10 catalysts are shown in Fig. 3. The grain size of CuO_X in Cu-Ti was found to be larger than those in Cu-Ti-BN-10, which was in line with the BET surface area results in Table 1.

3.3 XPS analysis

Fig. 4(a) shows the O 1s XPS spectra of CuO_X/TiO_2-hBN catalysts. The O1s peaks could be fitted into three peaks referred to the lattice oxygen (O^{2-}) at 529.7 eV (hereafter, denoted as O_β) and the chemisorbed oxygen (O_2^{2-} or O^-) belonging to defect-oxide at 531.1~531.7 eV (hereafter, denoted as O_α) [35-37]. The relative concentration ratio of $O_\alpha/(O_\alpha+O_\beta)$ ranked as follows: Cu-Ti-BN-15(37.5%)> Cu-Ti-BN-10(29.0%)> Cu-Ti-BN-5(28.5%)> Cu-Ti(25.5%). In addition, with the increase of BN concentration, the O_α peaks of CuO_X/TiO_2-hBN shifted to a higher binding energy (531.12 eV, 531.13 eV,

531.44 eV and 531.56 eV, respectively), which could facilitate the oxidation of NO to NO_2 on the surface of catalyst [36, 38]. Fig. 4(b) presents the Cu 2p XPS spectra of $CuOx/TiO_2$-hBN catalysts. The satellite peaks at 940.0-945.0 eV and 960.0-965.0 eV, and the other peaks of Cu are corresponded to the different copper oxides, namely, Cu^+ (932.8 and 952.6 eV) and Cu^{2+} (935.1 and 955.0 eV) [19, 21]. The relative intensity of $I_{Cu+}/ (I_{Cu+}+I_{Cu2+})$ of Cu-Ti-BN-10 (69.9%) is higher than that of Cu-Ti (64.5%), which could contribute to a higher NO_X reduction activity [35, 39, 40].

3.4 H_2-TPR and NH_3-TPD analysis

The H_2-TPR results are shown in Fig. 5(a) to investigate the reducibility over CuO_X/TiO_2-hBN catalysts. For Cu-Ti sample, four convoluted peaks detected could be ascribed to the sequential reduction of: (i) highly dispersed copper oxide species in close interaction with the support (139 °C), (ii) stepwise reduction of small and dispersed copper oxide to copper metallic (220 °C), (iii) the oxygen reduction of the support surface (395 °C) [16, 41]. Another broad peak at 493 °C could be ascribed to the reduction of bulk CuO, which is associated with bad dispersion of CuO_X on the support [41]. The almost disappearance of the peak at 493 °C for hBN supported catalysts indicates a good dispersion of CuO_X, in agreement with the SEM analysis.

The NH_3-TPD results are shown in Fig. 5(b). All the profiles display three peaks centered at about 129 °C, 198 °C and 245 °C, which could be attributed to the NH_3 desorbed by weak and medium acid sites. A same type of acid sites appears to be presented in these catalysts. From Fig. 5(b), the addition of hBN reduced the quantity of medium acid sites for NH_3 adsorption, especially for Cu-Ti-BN-5 and Cu-Ti-BN-10

as shown in Table 2.

3.5 NO-TPO and NO_X-TPD analysis

The SCR reaction rate can be substantially increased when a fraction of NO in the exhaust is converted to NO_2 [33, 42, 43]. Thus, the NO-TPO performance was studied and is shown in Fig. 6(a). The NO oxidation increased with temperature and reaches at a maximum value at about 375 °C due to the thermodynamic limits [44]. With the addition of hBN up to 10 wt%, the highest NO oxidation over each sample increased from 17.5% to 19.9%, and 24.7%, respectively. This indicated that hBN strengthened the oxidation activity of the catalysts. But it decreased to 18.8% when further adding hBN to 15 wt%.

The adsorption of NO_X species on the catalyst surface was also reported to play an important role in NO reduction [45]. Fig. 6(b) shows the NO_X (NO and NO_2) desorption profiles of these catalysts. The storage of NO_2 was observed to be much higher than that of NO over this series of catalysts. Moreover, Cu-Ti-BN-10 represented the best adsorption capacity of NO and NO_2 while Cu-Ti performed the worst. The signal of gaseous NO, detected over all the catalysts, showed two peaks at 100−200 °C and 200−300 °C attributed to physical and chemical adsorption, respectively. In addition, NO_2 desorption also represents two peaks, a weak peak at 150-250 °C and a strong at 250−350 °C. The NO_X-TPD results demonstrated that the addition of hBN promoted both the NO physical adsorption and NO_2 chemical adsorption on the catalyst surface. Fig. 6 indicated that NO especially NO_2 were mainly adsorbed on the catalyst surface during de-NO_X at temperature below 350 °C.

3.6 NH_3 Oxidation analysis

The selectivity in a SCR reaction is mainly governed by ammonia activation as the reaction temperature increases. However, over oxidation of NH_3 to NO_X are undesirable byproducts in a SCR reaction [31]. The NH_3 oxidation to NO_X during reaction is presented in Fig. 7, NH_3 conversion over all CuO_X/TiO_2-hBN catalysts kept at almost 0% below 250 °C, and then increased rapidly to 90% at 300 °C. while the NH_3 oxidation over Cu-Ti was evident at 250 °C, indicating a suppression of NH_3 oxidation by hBN. This was in agreement with the previous literatures [15, 31, 42]. In addition, the NO formation was also suppressed by hBN, as shown in Fig. 7(b). The NH_3 oxidation to NO reached to 22.8% over Cu-Ti at 300 °C compared to 6.8% over Cu-Ti-BN-15. Fig. 5 clearly indicated that the addition of hBN reduces the side reaction of NH_3 oxidation, which was beneficial to NO removal. Further addition of hBN (15%) increased the NH_3 oxidation to NO_X could be attributed to the high concentration of surface adsorbed oxygen species as shown in Fig. 4. As a result, the de-NO_X efficiency reduced as shown in Fig. 1. By the way, due to limitations of the instrument, the formation of N_2 and N_2O was not measured in this study.

3.7 Influence of SO_2 and H_2O on SCR activity

SO_2 and H_2O always exist in the exhaust even after the desulfurization and are detrimental to NO_X removal at low temperatures. The influence of SO_2 on the Cu-Ti-BN-10 catalyst at different temperatures was further investigated as shown in Fig. 8 (a).

The reaction temperature determines on deactivation behavior of SO_2. NO conversion decreased from 86% to 64% at 250 °C. With temperature increased, the SO_2 deactivation phenomena weakened. Moreover, the existence of SO_2 improved the SCR activity at 350 °C, which was in agreement with our previous studies [46]. Details of SO_2 influence was shown in Fig. 8 (b), NO conversion slightly decreased from 85% to 83% with 50 ppm SO_2 added, when SO_2 increased to 200 ppm, the NO conversion decreased to 58% within 80 min, and it recovered to 64% after SO_2 was switched off. The efficiency kept at 62-65% by 250 °C heating in N_2 for 1 h. This indicated that CuO_X based catalysts are easily deactivated by SO_2 [47]. Fortunately, after further heating the catalyst at 300 °C for 1h, the activity recovered back to its initial level.

The effect of H_2O on the de-NO_X activity over the Cu-Ti-BN-10 catalyst at 250 °C was further examined and shown in Fig. 9. When 10% H_2O was introduced into the system, the NO conversion decreased from 82% to 62% in 2 hours and then kept unchanged, but it recovered to the original level quickly after the H_2O was switched off. Even SO_2 was added at the same time, H_2O induced deactivation can also be recovered. So the de-NO_X efficiency decrease is mainly attributed to the competitive adsorption of H_2O and the reactant NH_3 [48].

The correlation among the performance of catalysts, the adsorption and oxidation behavior of NO and NH_3 could be established according to Fig. 1, 5, 6 and 7. The SCR reaction could be divided into four stages according to temperature as was discussed in Fig. 1. In Stage-1 for temperature below 150 °C, the catalysts showed low de-NO_X activity might due to the low NO and NH_3 activation as shown in Figs. 6 and 7 [32]. In

Stage-2 for temperature from 150 to 275 °C, the activation of NH_3 happened (Fig.7). Moreover, the NO to NO_2 oxidation was also promoted, which accelerated the SCR activity through the fast reaction of $2NH_3 + NO + NO_2 \rightarrow 2N_2 + 3H_2O$ [49, 50]. The different apparent activity energy in Stages-1 and -2 as shown in the inset of Fig. 1(b) and Table 2 supported this assumption. Because of the excessive oxidation of NH_3 (Fig. 7) and the decrease adsorptive capacity of NO and NO_2, the SCR activity began to decrease rapidly above 275 °C in Stage-3 at temperature from 275 to 350 °C. Finally in Stage-4 for temperature above 350 °C, NO_X were totally desorbed, and NO to NO_2 oxidation was minimized due to the thermodynamic limits. Moreover, the NH_3 oxidation became severe. All these could account for its low SCR performances. Note that, the increase of NO reduction efficiency below 275 °C (Fig. 1) is accompanied with adsorption of NO_2, indicating that the adsorbed NO_2 plays an important role for SCR activity [21]. Based on the discussion above, the NO_X reduction possibly follows the L-H mechanism through the reaction between NO_X adsorbed and NH_3 adsorbed at temperature below 350 °C [21].

4 Conclusions

In summary, we found that CuO_X/TiO_2 could be well dispersed over nitric acid treated hBN, and the SCR activity was significantly promoted especially with 10% hBN addition. The increased specific area, the promoted oxidation of NO to NO_2, the strong NO_X adsorption, and also the suppressed side reaction of NH_3 oxidation are all beneficial for NO_X conversion. High de-NO_X activities with a maximum conversion of 90.6% were achieved at 275 °C. Moreover, the regeneration of catalyst deactivation

caused by SO_2 at low temperature could be achieved by heating the catalyst at 300 °C, and SO_2 improved the SCR activity at 350 °C. Our study indicates that hBN is a promising catalyst promoter and carrier with excellent stability compared to carbonaceous materials.

Acknowledgements: This work was supported by the Environmentally Sustainable Management of Medical Wastes in China (Contract No. C/V/S/10/251), and the National Natural Foundation of Zhejiang Province, China (Grant No. Z4080070).

References:

[1] Z. Liu, S. Ihl Woo, Catalysis Reviews **2006**, 48, 43.

[2] A. Hornung, M. Muhler, G. Ertl, Catal. Lett., 1998, 53, 77.

[3] S. M. Park, M. Kim, E. S. Kim, H. Han, G. Seo, Appl. Catal. A: Gen., 2011, 395, 120.

[4] S. M. Park, H. Jang, E. S. Kim, H. Han, G. Seo, Appl. Catal. A: Gen., 2012, 427-428, 155.

[5] J. A. Sullivan, J. Cunningham, M. A. Morris, K. Keneavey, Appl. Catal. B: Environ., 1995, 7, 137.

[6] K. Rahkamaa-Tolonen, T. Maunula, M. Lomma, M. Huuhtanen, R. L. Keiski, Catal.Today, 2005, 100, 217.

[7] M. Iwasaki, K. Yamazaki, K. Banno, H. Shinjoh, J. Catal., 2008, 260, 205.

[8] L. Chmielarz, P. Kuśtrowski, A. Rafalska-Łasocha, D. Majda, R. Dziembaj, Appl. Catal. B: Environ., 2002, 35, 195.

[9] A. L. Kustov, S. B. Rasmussen, R. Fehrmann, P. Simonsen, Appl. Catal. B: Environ., 2007, 76, 9.

[10] R. Q. Long, R. T. Yang, J. Catal., 1999, 188, 332.

[11] R. Q. Long, R. T. Yang, J. Am. Chem. Soc., 1999, 121, 5595.

[12] Supriyanto, K. Wijayanti, A. Kumar, S. Joshi, K. Kamasamudram, N. W. Currier, A. Yezerets, L. Olsson, Appl. Catal. B: Environ., 2015, 163, 382.

[13] N. Wilken, K. Wijayanti, K. Kamasamudram, N. W. Currier, R. Vedaiyan, A. Yezerets, L. Olsson, Appl. Catal. B: Environ., 2011, 111-112, 58.

[14] W. B. Li, R. T. Yang, K. Krist, J. R. Regalbuto, Energy Fuel, 1997, 11, 428.

[15] J. H. Kwak, R. Tonkyn, D. Tran, D. Mei, S. J. Cho, L. Kovarik, J. H. Lee, C. H. F. Peden, J. Szanyi, ACS Catal., 2012, 2, 1432.

[16] S. Guerrero, I. Guzmán, G. Aguila, P. Araya, Catal. Commun., 2009, 11, 38.

[17] J. P. Espinós, J. Morales, A. Barranco, A. Caballero, J. P. Holgado, A. R. González-Elipe, J. Phys. Chem. B, 2002, 106, 6921.

[18] D. Pietrogiacomi, D. Sannino, S. Tuti, P. Ciambelli, V. Indovina, M. Occhiuzzi, P. Franco, Appl. Catal. B: Environ., 1999, 21, 141.

[19] Q. Li, H. Yang, Z. Ma, X. Zhang, Catal. Commun., 2012, 17, 8.

[20] J. Xiaoyuan, D. Guanghui, L. Liping, C. Yingxu, Z. Xiaoming, J. Mol. Catal. A: Chem., 2004, 218, 187.

[21] Z. X. Ma, H. S. Yang, Q. Li, J. W. Zheng, X. B. Zhang, Appl. Catal. A: Gen., 2012, 427, 43.

[22] O. V. Metelkina, V. V. Lunin, V. A. Sadykov, G. M. Alikina, R. V. Bunina, E. A. Paukshtis, V. B. Fenelonov, A. Y. Derevyankin, V. I. Zaikovskii, U. Schubert, J. R. H. Ross, Catal. Lett., 2002, 78, 111.

[23] N. M. Rodriguez, M. S. Kim, R. Baker, J. Phys. Chem., 1994, 98, 13108.

[24] S. Santucci, S. Picozzi, F. Di Gregorio, L. Lozzi, C. Cantalini, L. Valentini, J. M. Kenny, B. Delley, J. Chem. Phy.,2003, 119, 10904.

[25] G. Postole, M. Caldararu, N. I. Ionescu, B. Bonnetot, A. Auroux, C. Guimon, Thermochim. Acta., 2005, 434, 150.

[26] P. R. Kidambi, R. Blume, J. Kling, J. B. Wagner, C. Baehtz, R. S. Weatherup, R. Schloegl, B. C. Bayer, S. Hofmann, Chem. Mater., 2014, 26, 6380.

[27] Z. Liu, Y. Gong, W. Zhou, L. Ma, J. Yu, J. C. Idrobo, J. Jung, A. H. MacDonald, R. Vajtai, J. Lou, P. M. Ajayan, Nat. Commun., 2013, 4.

[28] C. Lin, J. Catal., 2002, 210, 39.

[29] G. Postole, A. Gervasini, M. Caldararu, B. Bonnetot, A. Auroux, Appl. Catal. A: Gen., 2007, 325, 227.

[30] Q. Li, H. Yang, A. Nie, X. Fan, X. Zhang, Catal. Lett., 2011, 141, 1237.

[31] S. Roy, B. Viswanath, M. S. Hegde, G. Madras, J. Phys. Chem. C, 2008, 112, 6002.

[32] G. Ramis, L. Yi, G. Busca, M. Turco, E. Kotur, R. J. Willey, J. Catal., 1995, 157, 523.

[33] J. H. Goo, M. F. Irfan, S. D. Kim, S. C. Hong, CHEMOSPHERE **2007**, 67, 718.

[34] X. Guo, C. Bartholomew, W. Hecker, L. L. Baxter, Appl. Catal. B: Environ., 2009, 92, 30.

[35] K. Sutthiumporn, S. Kawi, Int. J. Hydrogen. Energ., 2011, 36, 14435.

[36] L. Chen, J. Li, M. Ge, J. Chem. Eng., 2011, 170, 531.

[37] M. Kang, E. D. Park, J. M. Kim, J. E. Yie, Appl. Catal. A: Gen., 2007, 327, 261.

[38] Q. Li, H. S. Yang, F. M. Qiu, X. B. Zhang, J. Hazard. Mater., 2011, 192, 915.

[39] A. Sultana, T. Nanba, M. Haneda, H. Hamada, Catal. Commun., 2009, 10, 1859.

[40] C. Sun, J. Zhu, Y. Lv, L. Qi, B. Liu, F. Gao, K. Sun, L. Dong, Y. Chen, Appl. Catal. B: Environ., 2011, 103, 206.

[41] P. Larsson, A. Arne, J. Catal., 1998, 179, 72.

[42] S. Suárez, S. M. Jung, P. Avila, P. Grange, J. Blanco, Catal.Today, 2002, 75, 331.

[43] H. Wang, J. Wang, Z. Wu, Y. Liu, Catal. Lett., 2010, 134, 295.

[44] M. Devadas, O. Krocher, M. Elsener, A. Wokaun, N. Soger, M. Pfeifer, Y. Demel, L. Mussmann, Appl. Catal. B: Environ., 2006, 67, 187.

[45] M. Koebel, Catal.Today, 2002, 73, 239.

[46] Z. Ma, H. Yang, F. Liu, X. Zhang, Appl. Catal. A: Gen., 2013, 467, 450.

[47] Z. Zhu, Z. Liu, S. Liu, H. Niu, T. Hu, T. Liu, X. Yaning, Appl. Catal. B: Environ., 2000, 26, 25.

[48] Z. Huang, J. Catal., 2003, 214, 213.

[49] A. Kato, S. Matsuda, T. Kamo, F. Nakajima, H. Kuroda, T. Narita, J. Phy. Chem., 1981, 85, 4099.

[50] G. Tuenter, W. F. van Leeuwen, L. Snepvangers, Ind. Eng. Chem. Prod. Res. Dev. 1986, 25, 633.

Tables:

Table 1 Summary of the catalysts prepared via the sol–gel method.

Catalysts (A, B)[a]	hBN (wt%)	Surface Cu atomic concentration (%)[b]	S_{BET} (m^2/g)	Notation
CuO_X/TiO_2 (5.90, 0)	0	6.1	30.7	Cu-Ti
CuO_X/TiO_2-hBN (5.90, 1)	5	4.1	42.1	Cu-Ti-BN-5
CuO_X/TiO_2-hBN (5.90, 2)	10	4.5	78.1	Cu-Ti-BN-10
CuO_X/TiO_2-hBN (5.90, 3)	15	4.7	73.5	Cu-Ti-BN-15
pretreated hBN	-	-	22.4	BN

[a] The letter of A and B represent the measured mass of copper nitrate and hBN, respectively.

[b] Surface atomic concentration as calculated by XPS.

Table 2 Ea and NH_3 desorption peak area of the catalysts.

Notation	Ea from Fig.1(b)		Peak area from Fig.5(b)		
	100-175 °C	175-250 °C	100-150 °C	150-200 °C	200-300 °C
Cu-Ti	95.3	39.3	0.18	0.46	0.36
Cu-Ti-BN-5	43.2	34.8	0.34	0.42	0.24
Cu-Ti-BN-10	43.5	23.0	0.26	0.48	0.20
Cu-Ti-BN-15	57.9	31.9	0.25	0.43	0.30

Figures:

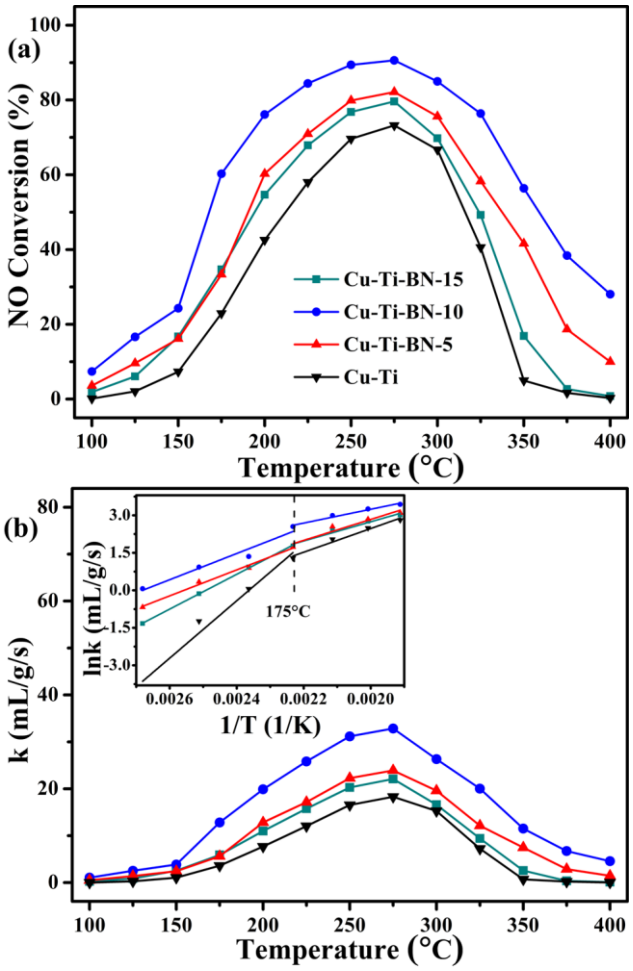

Fig. 1 (a) NO_X conversion over CuO_X/TiO_2-hBN catalysts. (b) The kinetic rate constant k over the catalysts. Reaction condition: $[NH_3]$ = 800 ppm, [NO] = 800 ppm, $[O_2]$ = 5.4%, balance N_2, and GHSV = 75,000 h^{-1}.

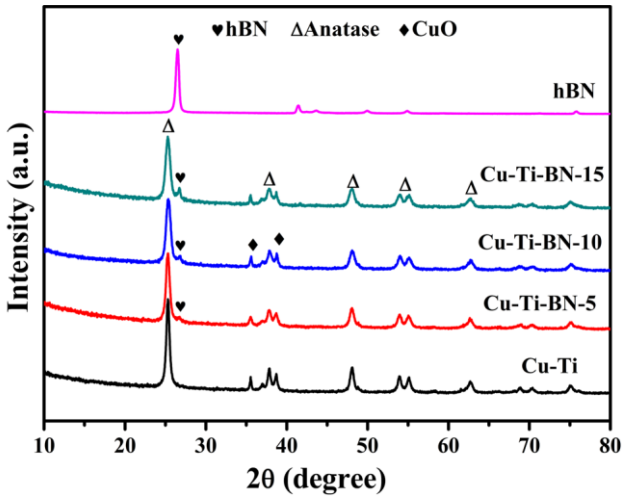

Fig. 2 XRD patterns of the hBN and CuO_X/TiO_2-hBN catalysts.

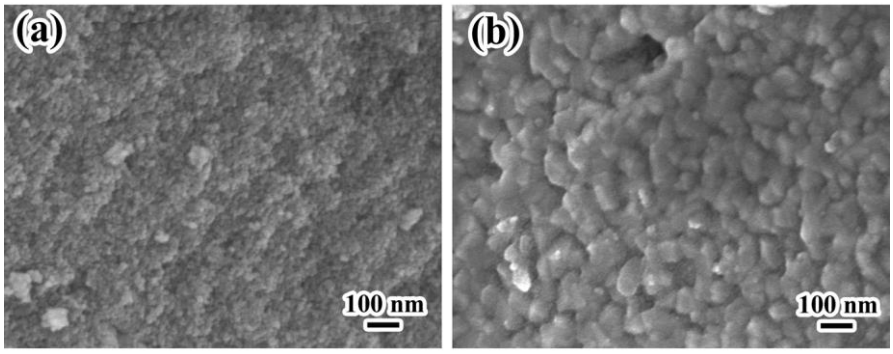

Fig. 3 SEM images of (a) Cu-Ti-BN-10; (b) Cu-Ti.

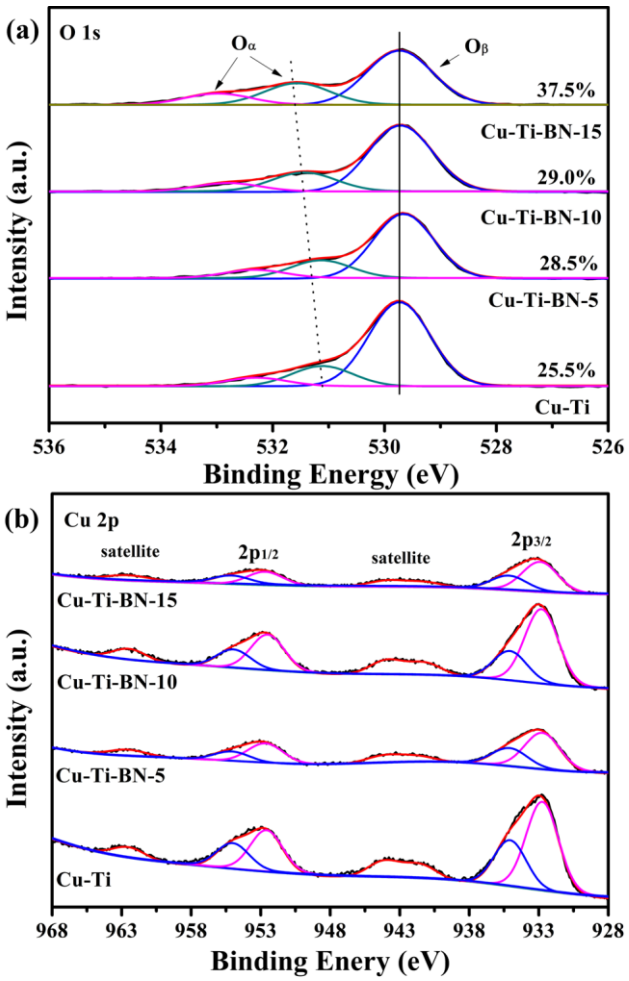

Fig. 4 XPS results of (a) O 1s and (b) Cu 2p in CuO_X/TiO_2-hBN catalysts.

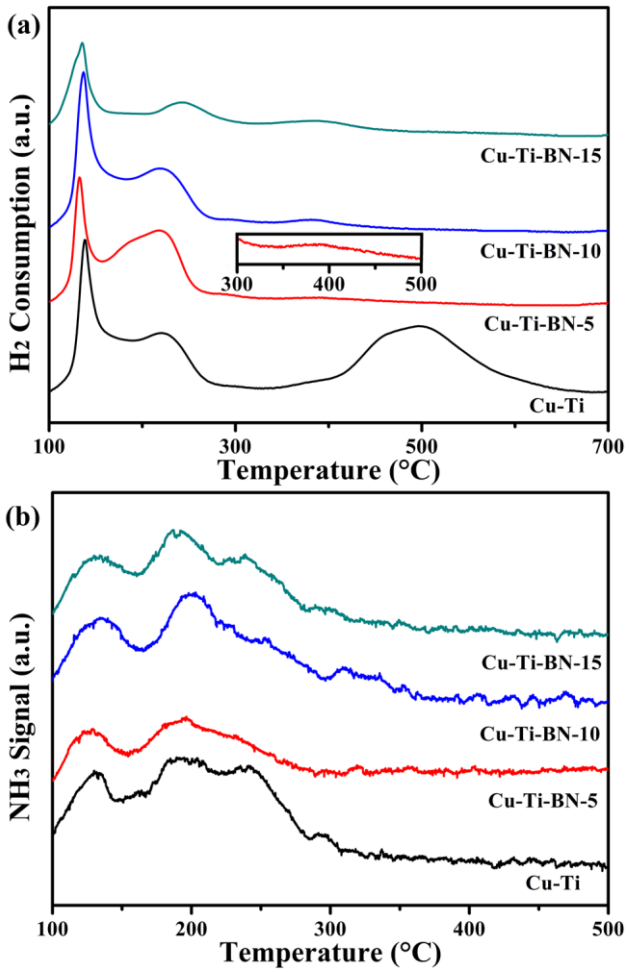

Fig. 5 (a) H_2-TPR and (b) NH_3-TPD profiles of the CuO_X/TiO_2-hBN catalysts.

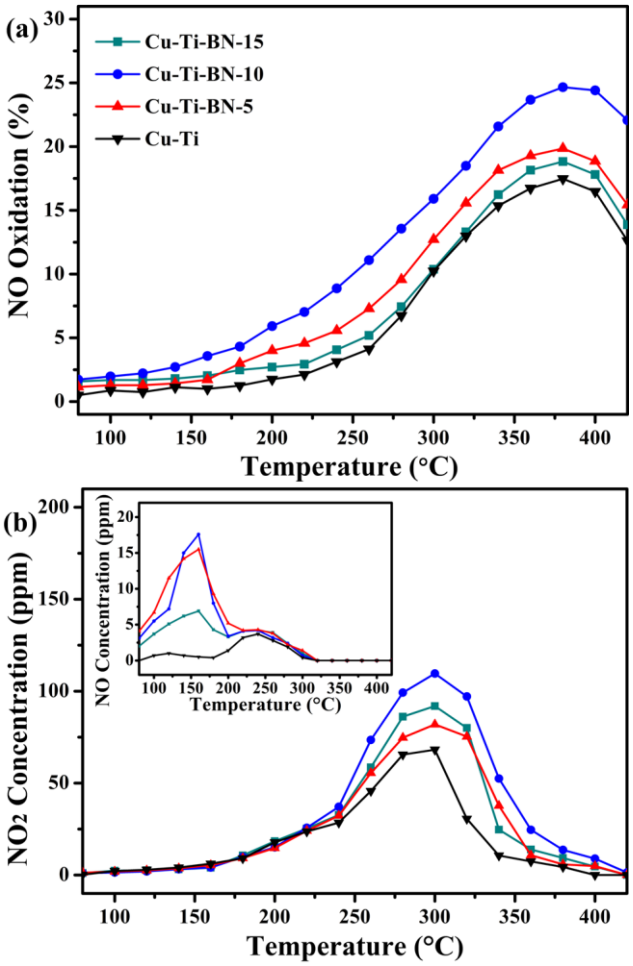

Fig. 6 (a) NO-TPO by O_2 over the CuO_X/TiO_2-hBN catalysts. Reaction conditions: [NO] = 800 ppm, [O_2] = 5.4%, balance N_2, and GHSV = 75,000 h^{-1}. (b) NO_X-TPD profiles of the CuO_X/TiO_2-hBN catalysts dosed with NO_X at 400 °C and then cooled to 100 °C in NO_X prior to temperature ramping.

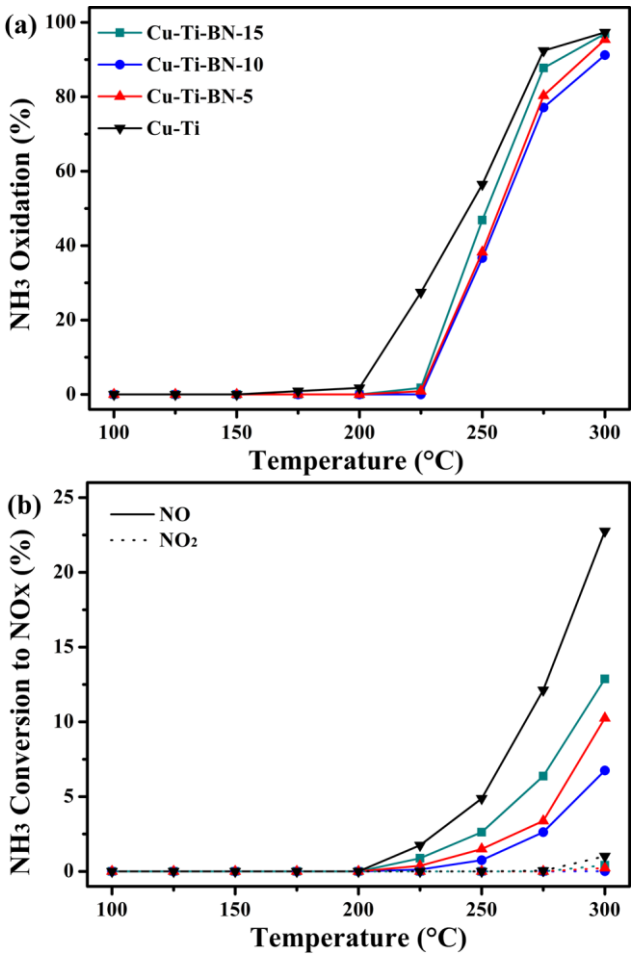

Fig. 7 NH_3-TPO by O_2 over CuO_X/TiO_2-hBN catalysts. Reaction conditions: [NH_3] = 800 ppm, [O_2] = 5.4%, balance N_2, and GHSV = 75,000 h^{-1}.NH_3-TPO profiles of the CuO_X/TiO_2-hBN catalysts dosed with NH_3 at 400 °C and then cooled to 100 °C in NO/O_2 prior to temperature ramping.

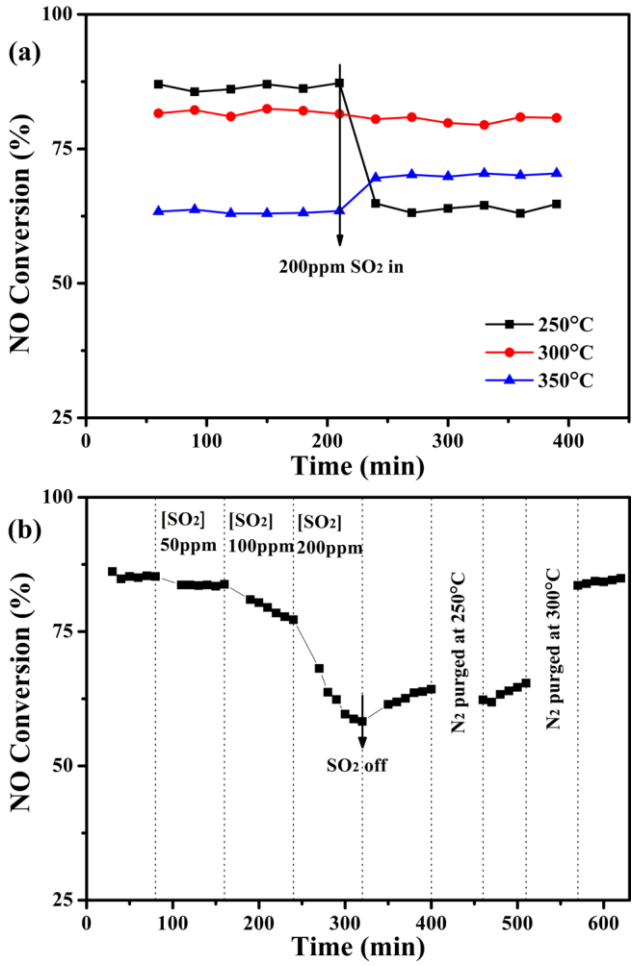

Fig. 8 (a) Effect of SO_2 on NO_X conversion over the Cu-Ti-BN-10 catalyst at different temperatures, reaction conditions: [NH_3] = 800 ppm, [NO] = 800 ppm, [O_2] = 5.4%, 200 ppm SO_2 (when used), balance N_2, and GHSV = 75,000 h^{-1}; (b) Effect of SO_2 concentration on NO_X conversion over Cu-Ti-BN-10 catalyst at 250 °C, reaction conditions: [NH_3] = 800 ppm, [NO] = 800 ppm, [O_2] = 5.4%, [SO_2] = 50-200 ppm (when used), balance N_2, and GHSV = 75,000 h^{-1}.

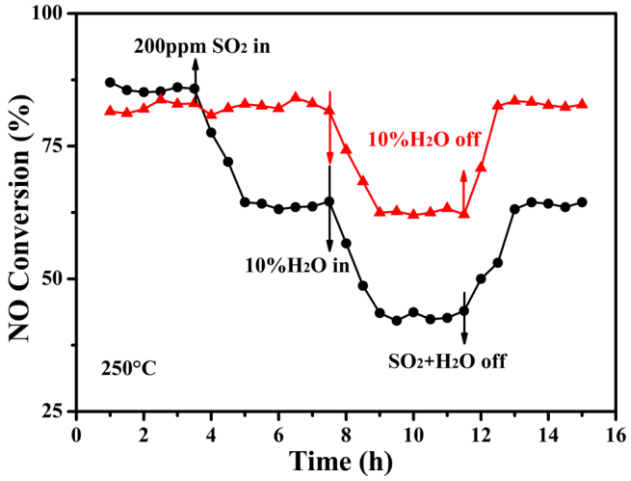

Fig. 9 Influence of H_2O on NO_X conversion over the Cu-Ti-BN-10 catalyst at 250 °C, reaction conditions: 200 ppm SO_2 and 10% H_2O (when used), [NH_3] = 800 ppm, [NO] = 800 ppm, [O_2] = 5.4%, balance N_2, and GHSV = 75,000 h^{-1}.